Biology Direct

RESEARCH

Open Access

ADAMTS4 exacerbates lung cancer progression via regulating c-Myc protein stability and activating MAPK signaling pathway

Wei Zhai[1†], Wensheng Yang[2†], Jing Ge[3†], Xuelian Xiao[4], Kang Wu[5], Kelin She[6], Yu Zhou[7], Yi Kong[7], Lin Wu[7], Shiya Luo[5] and Xingxiang Pu[7*]

Abstract

Background Lung cancer is one of the most frequent cancers and the leading cause of cancer-related deaths worldwide with poor prognosis. A disintegrin and metalloproteinase with thrombospondin motifs 4 (ADAMTS4) is crucial in the regulation of the extracellular matrix (ECM), impacting its formation, homeostasis and remodeling, and has been linked to cancer progression. However, the specific involvement of ADAMTS4 in the development of lung cancer remains unclear.

Methods ADAMTS4 expression was identified in human lung cancer samples by immunohistochemical (IHC) staining and the correlation of ADAMTS4 with clinical outcome was determined. The functional impact of ADAMTS4 on malignant phenotypes of lung cancer cells was explored both in vitro and in vivo. The mechanisms underlying ADAMTS4-mediated lung cancer progression were explored by ubiquitination-related assays.

Results Our study revealed a significant upregulation of ADAMTS4 at the protein level in lung cancer tissues compared to para-carcinoma normal tissues. High ADAMTS4 expression inversely correlated with the prognosis of lung cancer patients. Knockdown of ADAMTS4 inhibited the proliferation and migration of lung cancer cells, as well as the tubule formation of HUVECs, while ADAMTS4 overexpression exerted opposite effects. Mechanistically, we found that ADAMTS4 stabilized c-Myc by inhibiting its ubiquitination, thereby promoting the in vitro and in vivo growth of lung cancer cells and inducing HUVECs tubule formation in lung cancer. In addition, our results suggested that ADAMTS4 overexpression activated MAPK signaling pathway.

Conclusions We highlighted the promoting role of ADAMTS4 in lung cancer progression and proposed ADAMTS4 as a promising therapeutic target for lung cancer patients.

Keywords ADAMTS4, Lung cancer, c-Myc, Ubiquitination, Angiogenesis, MAPK signaling

[†]Wei Zhai, Wensheng Yang and Jing Ge have contributed equally to this work and share first authorship.

*Correspondence:
Xingxiang Pu
puxingxiang@hnca.org.cn
Full list of author information is available at the end of the article

Introduction

Lung cancer stands as one of the most frequent malignancies worldwide, responsible for a staggering number of cancer-related deaths, with nearly 2 million new cases reported annually [1]. It is categorized into non-small-cell lung cancer (NSCLC), which comprises approximately 85% of diagnoses, and small-cell lung cancer (SCLC), constituting the remaining 15% [2, 3]. Advancements in comprehending the disease's biology and controlling tobacco consumption have significantly contributed to reducing the incidence of lung cancer and improving patients' survival [4]. However, despite these strides, lung cancer continues to afflict individuals who have never smoked, and diagnoses often occur at advanced stages, hindering successful therapeutic intervention [5]. The standard treatment protocol for early-stage patients typically involves surgical resection combined with adjuvant chemotherapy, albeit accompanied by considerable toxicities [4, 6]. Furthermore, despite the targeted therapies and checkpoint immunotherapies hold promise in improving survival of both early and late–stage lung cancer patients [7, 8], numerous challenges persist. These include the modest efficacy of treatments and their applicability limited to a small subset of patients [9]. Therefore, large efforts are warranted to identify predictive biomarkers that could benefit a broader spectrum of lung cancer patients.

A disintegrin and metalloproteinase with thrombospondin motifs 4 (ADAMTS4) belongs to the zinc-dependent proteinase family, playing a pivotal role in the degradation of the extracellular matrix (ECM) and contributing significantly to the formation, homeostasis and remodeling of the ECM [10]. Both individual ECM proteins and entire families of ECM proteins serve as substrates for ADAMTS proteases [10, 11]. Mutations in ADAMTS proteases have been implicated in various diseases, including dermatosparaxis Ehlers Danlos syndrome, isolated heart valve disease, congenital thrombotic thrombocytopenic purpura and Alzheimer disease [12–14]. Moreover, dysregulation of ADAMTS4 has been linked to tumor progression. For instance, the upregulation of ADAMTS4 in colorectal cancer contributes to the tumor metastasis, angiogenesis and immunosuppression, potentially serving as a potential prognostic indicator for colorectal cancer [15, 16]. Similarly, ADAMTS4 is highly expressed in patients with Ewing's sarcoma, suggesting its potential as a novel tumor maker for this type of cancer [17]. Additionally, Rao et al. demonstrated that both full-length ADAMTS4 and its N-terminal 53 kDa autocatalytic fragment promote B16 melanoma growth and angiogenesis in mice [18]. However, the biological role of ADAMTS4 in lung cancer remains unidentified. Investigating the underlying mechanism of ADAMTS4 in lung cancer may offer an attractive therapeutic target.

C-Myc encodes a transcription factor that regulates the expression of numerous target genes involved in essential cellular processes such as proliferation, differentiation, and apoptosis [19]. It consists of several functional domains, including a basic helix-loop-helix (bHLH) domain that mediates DNA binding, a leucine zipper domain for dimerization with Max protein, and a transactivation domain responsible for activating target gene expression [20]. The activity of c-Myc is tightly regulated at multiple levels, including transcriptional, post-transcriptional, and post-translational mechanisms [21, 22]. Aberrant activation of c-Myc, often through gene amplification or chromosomal translocation, is associated with various cancers, where it drives abnormal cell growth and proliferation [23–25]. C-Myc overexpression in cancer cells correlates with poor prognosis and resistance to therapy [26]. Consequently, c-Myc has emerged as a significant therapeutic target, with ongoing efforts to develop drugs that inhibit its activity or downstream signaling pathways, aiming to improve treatment outcomes for cancer patients.

In this study, we identified the upregulation of ADAMTS4 in lung cancer, correlating with a poor prognosis for patients. Moreover, ADAMTS4 was confirmed to promote lung cancer cells proliferation and migration, and this effect was dependent on c-Myc. Mechanistically, ADAMTS4 regulated protein stability of c-Myc by ubiquitin–proteasome system (UPS) and activated the MAPK signaling pathway, thereby promoting lung cancer progression. These findings indicated a potential avenue for targeted therapies in lung cancer by modulating the ADAMTS4/c-Myc axis.

Materials and methods

Clinical tissue specimens and immunohistochemical (IHC) staining analysis

The human microarray, composed of 149 lung cancer tissues and 88 para-carcinoma normal tissues, was used to assess expression of ADAMTS4 by IHC staining. Detailed clinicopathologic information for each patient was available. The process of IHC staining involved dewaxing the embedded tissues at 65 °C, followed by treatment with xylene and gradient alcohol. Antigen using EDTA buffer and blocking of endogenous peroxidase using 3% H_2O_2 were then performed. The prepared tissue slides were incubated overnight at 4 °C with primary antibody anti-ADAMTS4, followed by incubation with the corresponding secondary antibody at 37 °C for 1 h. The specific details of the antibodies used can be found in Table S1. Post-antibody incubation, the tissue

were stained with diaminobenzene (DAB), counterstained with hematoxylin, sealed with neutral gum, and subjected to subsequent scoring. Two independent histopathologists completed the assessment of IHC staining, and the ADAMTS4 IHC score was determined as the product of percentages of positive staining cells and the staining intensity. The former was graded as follows: 1, 0 ~ 24%; 2, 25 ~ 49%; 3, 50 ~ 74%; 4, 75 ~ 100%, while the latter was graded as: 0, no staining signals; 1, light yellow; 2, pale brown; 3, seal brown. The final IHC scores were determined as: 0 score (-), 1–4 scores (+), 5–8 scores (++), 9–12 scores (+++) [27].

Cell culture

The normal human lung epithelial cell BEAS-2B, along with human lung cancer cell lines A549, NCI-H1299, NCI-H1975, and human umbilical vascular endothelial cells (HUVECs), were obtained from the American Type Culture Collection (ATCC) (Manassas, USA). All cell lines were cultured in DMEM medium (Gibco, USA) supplemented with 10% fetal bovine serum (FBS) (Gibco, USA) and 1% Penicillin/Streptomycin (100 U/mL). The cells were maintained in a 5% CO_2 incubator at 37 °C.

RNA interference and overexpression

The ADAMTS4 overexpressing vector (ADAMTS4), ADAMTS4 silencing vector (shADAMTS4), and c-Myc silencing vector (shc-Myc) as well as the overexpressing scrambling vector (NC) and silencing negative control vector (shCtrl) were constructed according to the manufacturer's protocol. The targeted sequences of shRNAs were shown in Table S2. The RNA interference sequence was synthesized following a specific design and inserted into lentiviral BR-V108 vector (YiBR, China). The plasmids carrying the targeted interference sequence were then transduced into *Escherichia coli* (Cat. #CB104-03, TIANGEN), and the positive cloned plasmids were screened subsequently. Afterwards, the recombinant lentivirus plasmids (shADAMTS4 and shc-Myc) were generated by co-transfecting validated plasmids with pMD2.G (Qiagen, China) and pSPAX2 (Qiagen, China) packaging plasmids into HEK293T cells. Similarly, the recombinant lentivirus containing the amplified sequence of ADAMTS4 (ADAMTS4 overexpression) was accomplished as above generation of shRNA lentivirus. For lentiviral transfection, A549 and NCI-H1299 cells were seeded into 6-well plate at a density of 2×10^5 cells per well and then exposed to 10 μg of the indicated lentivirus. The stable overexpressing and knockdown cell lines were selected using puromycin, as previously described [28].

Real-time quantitative PCR (qPCR)

The total RNA from each cellular specimen was isolated using TRIzol regent (Sigma, USA), followed by RNA quantification using Nanodrop 100 (Thermo, USA). Subsequently, the prepared total RNA was reverse-transcribed into cDNA following the manufacturer's instructions for the Hiscript QRT supermix Kit (Vazyme, China). For the amplification of targeted genes, 10 μL of cDNA template was added according to the protocol of SYBR Green mastermixs Kit (Vazyme, China) using the Biosystems 7500 Sequence Detection system. The relative expression of targeted genes was calculated using the $2^{-\Delta\Delta Ct}$ method after normalization with internal control GAPDH. Each experiment was performed in triplicate. Primer sequences used here were listed in Table S3.

Western blotting (WB)

Total cellular proteins were extracted using radioimmunoprecipitation (RIPA) lysis, and their concentrations were determined with the BCA Protein Assay Kit (HyClone-Pierce, USA). The proteins were then separated by 10% sodium dodecyl sulfate polyacrylamide gel electrophoresis (SDS-PAGE) (Invitrogen, USA) followed by transferring onto polyvinylidene difluoride (PVDF) membranes. Subsequently, the membranes were incubated overnight at 4 °C with indicated primary antibodies, following a 1-h blocking step with 5% slim milk. After that, the membranes were incubated with a secondary antibody conjugated with horseradish peroxidase (HRP) at 37 °C for 2 h. Protein bands were visualized using enhanced chemiluminescence (ECL, Millipore). GAPDH was used as a loading control. Details of all antibodies used in WB analysis are provided in Table S1.

Cell proliferation assay

The cell viability of A549 and NCI-H1299 cells were determined using Celigo cell counting assays and CCK-8 assays. Following transfection with indicated lentivirus for 48 h, the cells were harvested and seeded into 96-well plates at a density of 2×10^3 cells per well, and then cultured for 5 consecutive days. Cell viability was assessed by quantifying the cell number using the Celigo image cytometer (Nexcelon Bioscience) at indicated time points. Additionally, for CCK-8 assays, the transfected cells were seeded into 96-well plates at a density of 5×10^3 cells per well and for 5 consecutive days. Subsequently, the absorbance of the cells at 450 nm was determined by microplate reader (Thermo, USA) after incubation with the CCK-8 solution.

Apoptosis assay

The flow cytometry was utilized for cell apoptosis analysis. A549 and NCI-H1299 cells, which were either expressing shADAMTS4 lentivirus or its negative control vector, were firstly harvested and then resuspended in 1 × PBS. Subsequently, Annexin V-APC (BD Biosciences, USA) and propidium iodide (PI) was added to the cell suspension and incubated in the dark for 15 min. Following staining, the cells were resuspended in 1 × binding buffer and washed 3 times with 1 × PBS. Finally, the prepared cells were analyzed using fluorescence-activated cell sorting (FACS) with a flow cytometer (Millipore, USA). The percentages of apoptotic cells were determined as Annexin-V/PI positive staining cells.

Wound healing assay

A549 and NCI-H1299 cells expressing shADAMTS4 lentivirus or its negative control vector were collected at 80% confluence. Subsequently, the cell density was adjusted to 5×10^4 cells/mL, and 100 μL of cell suspension was added into each well of 96-well plates. The next day, parallel scratches were made in each well using scratch tester when cells reached 90% density. A serum-free medium was then prepared and added to the plates to remove exfoliated cells. After that, the cells were supplemented with 0.5% FBS-containing medium for continuted cultivation until indicated time points. Finally, the migratory distance of cells was determined using Cellomics (Thermo, USA), and the migration rate was calculated based on the migratory distance.

Transwell assay

The transwell assay kit (Corning, USA) was used for assessing ability of cell migration, and the experiments were carried out according to its protocol. A549 and NCI-H1299 cells transfected with shADAMTS4 lentivirus or its negative control vector were harvested and re-suspended in FBS-free medium. The lower chambers were filled with medium supplemented with 30% FBS, while 100 μL of cell suspensions were added into the upper chamber. After 24 h of incubation at 37 °C with 5% CO_2, the migratory cells were fixed with 4% paraformaldehyde for 30 min and stained with 0.1% crystal violet for 10 min. Subsequently, migratory cells were counted under a light microscope (Olympus, Japan) in 5 fields selected from each well. Each experiment was performed in triplicate.

Bioinformatics analysis

The co-expressed genes with ADAMTS4 were identified using Coexpedia (https://www.coexpedia.org). Higher likelihood scores (LLS) represent the greater possibility of co-expression. The co-expression correlation for ADAMTS4 and MYC in LUAD was performed using starbase (http://starbase.sysu.edu.cn). The expression data of LUAD were downloaded from TCGA project (https://www.cancer.gov) via Genomic Data Commons Data Portal (https://portal.gdc.cancer.gov/). The expression values of genes from RNA-seq data were scaled with log2(FPKM + 0.01). The overall survival (OS) curve of ADAMTS4 in lung cancer was generated based on Kaplan–Meier method. The potential signaling pathway activated by ADAMTS4 was analyzed through Gene set enrichment analysis (GSEA, http://software.broadinstitute.org/gsea/msigdb/index.jsp) software based on the TCGA-LUAD dataset.

Protein stability assay

A549 and NCI-H1299 cell lines were transfected with a lentivirus carrying shADAMTS4 or its corresponding negative control. These cells were then plated in 12-well plates at a concentration of 10^5 cells per well. Following a 48-h incubation period, the cells underwent treatment with 100 μmol/L cycloheximide (CHX) (C7698, Sigma) for specified durations. Subsequently, cell samples were harvested and subjected to Western blot analysis using a c-Myc antibody.

Immunoprecipitation analysis

To conduct immunoprecipitation, A549 and NCI-H1299 cells, which were stably transfected with shADAMTS4 or shCtrl, underwent lysis using RIPA lysis buffer. The resulting cell lysate was then combined with either c-Myc-conjugated beads or IgG-conjugated beads, followed by an overnight incubation at 4 °C. Subsequently, the immunocomplexes were separated from the beads through centrifugation and subjected to Western blot analysis using an ubiquitin antibody.

Ubiquitination assay

Ubiquitination assays were performed as described previously [29]. In brief, cells were transfected with the shCtrl or shADAMTS4 lentivirus and incubated for 48 h. Subsequently, the cells were harvested following treatment with 20 μg/mL MG132 for 5 h. The cell lysates were then prepared using RIPA buffer and denatured by boiling for 5 min. The ubiquitination status of c-Myc was determined by western blot analyses, employing the methods described earlier.

HUVEC tube formation assay

The tubule formation assays of HUVECs were performed as described previously [30]. Briefly, 150 μL of growth factor-reduced Matrigel (BD Biosciences, USA) was added into 48-well plates for 30 min at 37 °C. HUVEC

cells, which had been starved in 0.2% FBS-containing DMEM medium for 24 h, were then digested and harvested. Moreover, culture medium (CM) from A549 and NCI-H1299 cells transfected with indicated lentivirus was collected. The cell density of HUVEC cells was adjusted to 1×10^5 cells/mL and re-suspended in corresponding CM. Subsequently, 500 μL of cell suspension was added to each well of the 48-well plates and incubated in an incubator for 7 h. Finally, the formed tubes were quantified by measuring the branch points of the completed tubules under a bright-field microscope (Olympus, Japan). Three independent experiments were performed for each treatment.

Mice xenograft model

BALB/c nude mice (female, eight-weeks-old) were purchased from GemPharmatech Co. LTD (Jiangsu, China). A549 cells transfected with ADAMTS4-ovexpressing or (and) shc-Myc lentivirus were subcutaneously injected to corresponding mice to construct xenograft models. 7 days later, the tumor sizes, including the widest diameter (W) and the longest diameter (L) of the mice tumors, were monitored every 6 days, and the tumor volumes were calculated using the formula $\pi/6\times L\times W^2$ [31]. After 31 days, all mice were anesthetized, and the tumor tissues were isolated, photographed, and weighted. Additionally, the tumor tissues were embedded in paraffin, and sectioned for Ki-67 staining as described above. The animal experiments were approved by the Institutional Animal Care Committee of Hunan Cancer Hospital/the affiliated Cancer Hospital of Xiangya school of Medicine, Central South University.

Statistical analysis

Graphpad Prism 8.04 software was used to perform statistical analysis and graphing. All data were expressed as the mean ± standard deviations (SD). Statistical differences were determined by unpaired two-tailed student's *t*-test and one-way analysis of variance (ANOVA). A p value of less than 0.05 was considered significantly difference.

Results

Increased ADAMTS4 expression in lung cancer predicted poor patient survival

To reveal whether ADAMTS4 expression is increased in lung cancer, we detected the ADMATS4 expression in lung cancer tissues (n = 149) and para-carcinoma normal tissues (n = 88) using human tissue microarrays via IHC staining. We revealed a significantly elevated level of ADMATS4 expression in lung cancer tissues compared to para-carcinoma normal tissues ($p < 0.001$) (Fig. 1A, B). The rate of positive ADMATS4 expression in lung cancer patients was 50.3% (75/149), markedly higher than the 3.4% (3/85) observed in para-carcinoma normal tissues ($p < 0.001$) (Table 1). To explore the role of ADMATS4 overexpression in lung cancer progression, we performed the correlation analysis between ADMATS4 expression and clinicopathological characteristics of lung cancer patients. The data suggested a significant correlation between high ADMATS4 expression and tumor stage, T infiltrate and lymphatic metastasis ($p < 0.05$) (Table 2). These positive correlations were further validated by Spearman correlation analysis (Table 3). Furthermore, patients with high ADAMTS4 expression showed apparent shortened overall survival (OS) in comparison with low ADAMTS4 expression (Fig. 1C). Collectively, these results indicated a substantial upregulation of ADAMTS4 in lung cancer tissues. The overexpression of ADAMTS4 is indicative of advanced disease progression and is associated with poor overall survival. Thus, ADAMTS4 holds promise as a potential prognostic biomarker for lung cancer progression.

ADAMTS4 knockdown inhibited proliferation, migration and angiogenesis in lung cancer

In consistent with the IHC results of human samples, we also bserved the overexpression of ADAMTS4 in lung cancer cell lines, such as NCI-H1299, NCI-H1975 and A549 ($p < 0.05$) (Fig. 1D, E). To investigate the biological functions of ADAMTS4 in lung cancer pathogenesis, a serious of loss-of-function experiments were performed using ADAMTS4-silencing cell models. Specifically, three ADAMTS4 interference lentiviral vectors (shADAMTS4) and a negative control (shCtrl) were constructed. The most effective shRNA targeting ADAMTS4 (shADAMTS4-2) was used for ADAMTS4 knockdown in A549 and NCI-H1299 lung cancer cells (Fig. S1A). Successful knockdown of ADAMTS4 was confirmed at both mRNA and protein levels ($p < 0.05$) (Fig. 2A, B). We first evaluated the effects of ADAMTS4 on proliferation and apoptosis by Celigo cell count assays and flow cytometry assays, respectively. Our results suggested that ADAMTS4 knockdown significantly inhibited the proliferation of A549 and NCI-H1299 lung cancer cells compared to the shCtrl group ($p < 0.001$) (Fig. 2C). Whereas, the percentages of cell apoptosis in shADAMTS4 group were obviously increased compared to the shCtrl group, with consistent results obtained in both A549 and NCI-H1299 cells ($p < 0.01$) (Fig. 2D). Given the association of ADAMTS4 upregulation with tumor progression and lymphatic metastasis, we examined whether ADAMTS4 promoted migration of lung cancer cells. Wound healing and transwell assays revealed that ADAMTS4 knockdown significantly decreased the migration rate and the number of migratory cells in both A549 and NCI-H1299

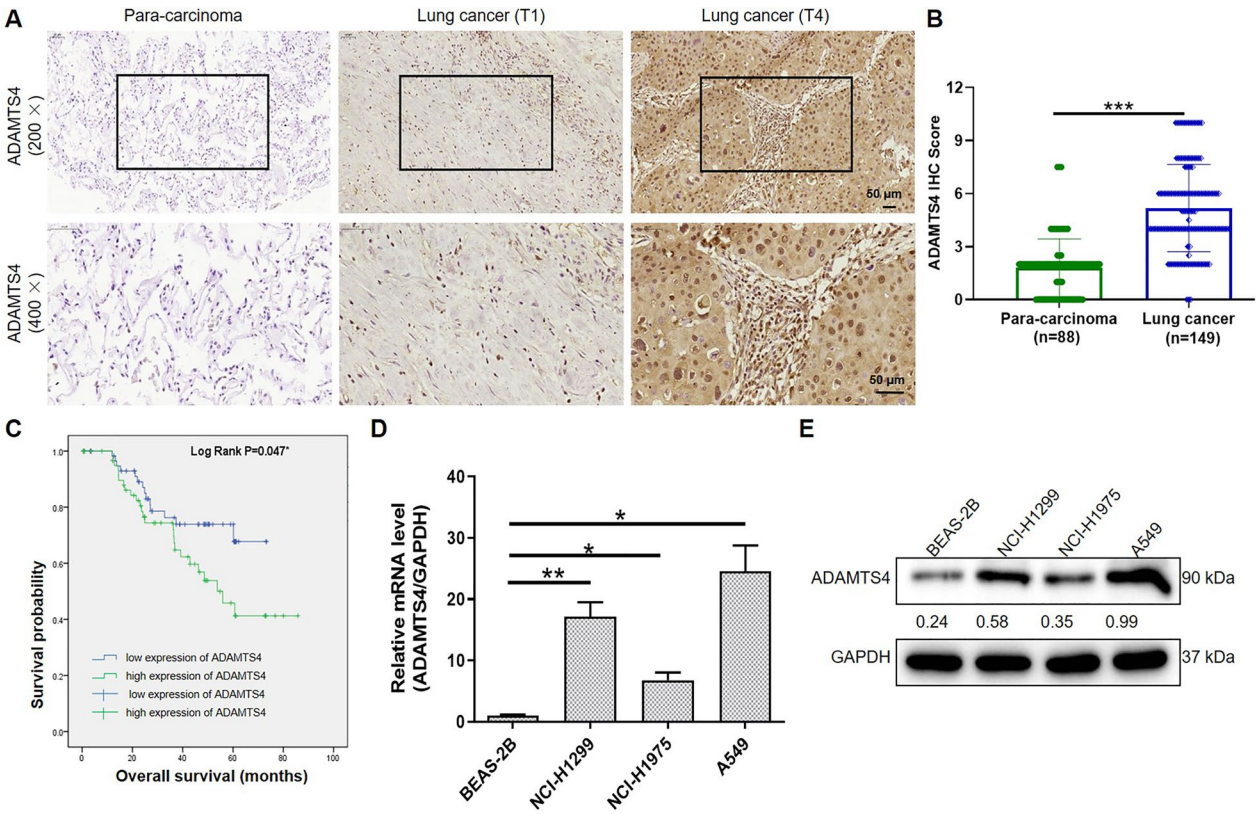

Fig. 1 Increased ADAMTS4 expression in lung cancer predicted poor patient survival. **A** Representative IHC images of analysis ADAMTS4 expression in human lung cancer tissues and para-carcinoma normal tissues. Scale bar: 50 μm. **B** The IHC score of ADAMTS4 from patients in lung cancer and para-carcinoma normal tissues. **C** Patients with high ADAMTS4 expression (n = 75) showed significantly shortened OS compared to that with low ADAMTS4 expression (n = 74). **D** Relative mRNA and (E) protein expression levels of ADAMTS4 in lung cancer cell lines NCI-H1299, NCI-H1975, A549 and normal lung epithelial cell BEAS-2B. (n = 3). Results were presented as mean ± SD. *$p < 0.05$, **$p < 0.01$, ***$p < 0.001$

Table 1 Expression of ADAMTS4 in lung cancer tissues and para-carcinoma normal tissues were revealed by immunohistochemistry analysis

ADAMTS4 expression	Tumor tissue		Para-carcinoma normal tissue		*p* value
	Cases	Percentage (%)	Cases	Percentage (%)	< 0.001
Low	74	49.7	85	96.6	
High	75	50.3	3	3.4	

cells compared to the negative control ($p < 0.05$) (Fig. 2E, F). This indicates that ADAMTS4 depletion impaired migratory capacities of lung cancer cells. Considering the reported involvement of ADAMTS4 in angiogenesis in cancers [18], and recognizing angiogenesis as a crucial step in driving progression of lung cancer [32], we sought to explore whether ADAMTS4 regulates angiogenesis in lung cancer. Since many angiogenic factors are soluble, we collected conditioned medium (CM) from both the shCtrl group of A549 and NCI-1299 cells and the shADAMTS4 group of A549 and NCI-1299 cells. We then examined their effects on the tube formation of HUVEC. We found that CM from ADAMTS4 knockdown A549 and NCI-1299 cells significantly reduced HUVECs tubule formation, implying a promoting role of ADAMTS4 in lung cancer angiogenesis (Fig. 2G).

To further confirm the influence of ADAMTS4 on the apoptotic, migratory and angiogenic phenotypes of lung cancer cells, the related protein expression levels were evaluated by western blot assays. As depicted in the Fig. 2H, when comparing the ADAMTS4 knockdown group with the control group, we observed a significant upregulation in the expression of pro-apoptotic proteins, Cleaved caspase-3 and Bax. Concurrently, there was a downregulation of the anti-apoptotic protein Bcl-2. Additionally, we found a marked decrease in the expression levels of pro-angiogenic proteins VEGF and PDGFA, as well as pro-migratory proteins MMP-1, Vimentin, and N-cadherin. These findings collectively reinforce our conclusion that ADAMTS4 plays a pivotal role in influencing

Table 2 Relationship between ADAMTS4 expression and tumor characteristics in patients with lung cancer

Features	No. of patients	ADAMTS4 expression		*p* value
		Low	High	
All patients	149	74	75	
Age (years)				0.564
< 62	70	33	37	
≥ 62	79	41	38	
Gender				0.965
Male	115	57	58	
Female	34	17	17	
Tumor size				0.222
< 3.5 cm	71	39	32	
≥ 3.5 cm	78	35	43	
Grade				0.374
II	42	24	18	
III	20	9	11	
Stage				< 0.01
I	54	35	19	
II	59	29	30	
III	25	7	18	
IV	8	3	5	
T Infiltrate				< 0.05
T1	71	39	32	
T2	40	22	18	
T3	16	9	7	
T4	2	4	18	
Lymphatic metastasis (N)				< 0.05
N0	78	45	33	
N1	54	26	28	
N2	14	3	11	
Metastasis				0.481
M0	141	71	70	
M1	8	3	5	

Table 3 Spearman correlation analysis between ADAMTS4 expression and tumor characteristics in patients with lung cancer

		ADAMTS4
Stage	Spearman correlation	0.254
	Significance (two-tailed)	< 0.01
	N	146
T Infiltrate	Spearman correlation	0.169
	Significance (two-tailed)	< 0.05
	N	149
Lymphatic metastasis (N)	Spearman correlation	0.182
	Significance (two-tailed)	< 0.05
	N	146

apoptosis, angiogenesis, and cell migration in lung cancer cells. Taken together, these findings reminded the potential of ADAMTS4 to promote the development of lung cancer via enhancing cell proliferation, migration and angiogenic ability while inhibiting cell apoptosis.

ADAMTS4 knockdown induced the degradation of c-Myc by ubiquitination in lung cancer

To identify the functional partners of ADAMTS4, we performed a prediction using Coexpedia and identified proteins exhibiting co-expression. As shown in Fig. 3A, the co-expression of ADAMTS4 with TRIM16L, CACNG4, WFDC9, BHLHE40, BRIX1, MYC, P4HA3, TBXA2R and NPAP1 had higher likelihood scores (LLS), indicating the probable co-expression of these genes. Notably, among the candidates, MYC is well recognized as an oncoprotein that regulates the expression of numerous genes implicated in cell survival, proliferation, apoptosis and metabolic pathways [33]. According the correlation analysis from ENCORI (https://rna.sysu.edu.cn/encori/panGeneCoExp.php), we found a positive association between MYC and ADAMTS4 in lung adenocarcinoma (LUAD) ($p < 0.001$) (Fig. 3B). Moreover, both NCI-H1299 and A549 cells showed a higher expression level of MYC compared to normal BEAS-2B cells ($p < 0.01$) (Fig. 3C). Further, we investigated whether ADAMTS4 regulated MYC expression by qPCR and western blot analysis. Our results showed that ADAMTS4 deficiency apparently suppressed mRNA and protein expression levels of c-Myc in A549 and NCI-H1299 cells, implying the regulatory role of ADAMTS4 in c-Myc expression (Fig. 3D, E). Most importantly, we noticed the crucial role of the ubiquitin–proteasome system (UPS) in regulating MYC protein levels in human cancers [34]. This led us to infer that ADAMTS4 affects the expression of MYC protein by regulating its ubiquitination level. Subsequently, we performed the cycloheximide (CHX) chase assays and monitored c-Myc expression by WB assays at indicated time points to evaluate whether ADAMTS4 mediates c-Myc deubiquitination. The results revealed that ADAMTS4 knockdown markedly decreased the half-life of c-Myc protein in A549 and NCI-H1299 cells (Fig. 3F). In addition, the downregulation of c-Myc was significantly reversed in ADAMTS4 knockdown A549 and NCI-H1299 cells treated with MG132, an inhibitor of ubiquitin–proteasome pathway, indicating that ADAMTS4 may regulate c-Myc protein stability through UPS (Fig. 3G). Next, we employed Ubibrowser (http://ubibrowser.bio-it.cn/) and String (https://cn.string-db.org/) websites to screen for potential interaction partners of ADAMTS4, particularly focusing on E3 ubiquitin ligase of c-Myc. We found that WWP2 was the only E3 ubiquitin ligase that may interact with ADAMTS4 (Fig. 4A). The endogenous

interaction among ADAMTS4, c-Myc and WWP2 in A549 and NCI-H1299 cells was confirmed by Co-IP analysis (Fig. 4B). Moreover, CHX chase assays demonstrated that increased WWP2 expression significantly accelerated c-Myc protein degradation (Fig. 4C). WWP2 overexpression decreased c-Myc protein levels in A549 and NCI-H1299 cells, while this effect was abolished by MG132 exposure (Fig. 4D). These results indicated that WWP2 degraded c-Myc by promoting UPS. Consistently, the ubiquitination assay suggested that ADAMTS4 overexpression greatly reduced the ubiquitination of c-Myc in A549 and NCI-H1299 cells. This effect was attenuated when WWP2 is co-overexpressed simultaneously. (Fig. 4E). Therefore, we inferred that ADAMTS4 may upregulate c-Myc expression by inhibiting WWP2-mediated c-Myc ubiquitination.

The function of ADAMTS4 in promoting proliferation, migration and angiogenesis relied on c-Myc

Since ADAMTS4 regulats protein levels of c-Myc, we hypothesized that c-Myc was essential for ADAMTS4 induced malignant behaviors of lung cancer cells. Consequently, we conducted the rescue experiments to examine this assumption. We employed shc-Myc-2, which exhibited satisfactory knockdown efficiency, for subsequent functional studies in A549 and NCI-H1299 cells (Fig. S1B). As depicted in Fig. 5A, western blot results confirmed the protein expressions of ADAMTS4 and c-MYC in both A549 and NCI-H1299 cells. The data revealed a significant increase in the protein levels of ADAMTS4 and c-MYC in the ADAMTS4 overexpression group compared to the control group. Conversely, in the c-Myc knockdown group, there was a noticeable reduction in c-MYC protein levels, with no significant change observed in ADAMTS4 levels. These results substantiated the successful overexpression and knockdown of ADAMTS4 and c-MYC, respectively, and support the conclusion that ADAMTS4 acts as an upstream regulator of c-MYC. Subsequently, cell proliferation and cell migration were detected. In CCK-8 assays, we found that the depletion of c-Myc significantly attenuated the effects on cell viability promoted by ADAMTS4 overexpression in A549 and NCI-H1299 cells ($p < 0.01$) (Fig. 5B). Moreover, the results of transwell assays suggested that the migratory capacity in ADAMTS4 group of A549 and NCI-H1299 cells was remarkably increased ($p < 0.001$), while it was dramatically suppressed in shc-Myc and ADAMTS4 + shc-Myc groups as compared with the matched control groups ($p < 0.001$) (Fig. 5C). In the tubule formation assay, we observed that CM from ADAMTS4-overexpressing cells enhanced the capillary formation of HUVECs, while CM from c-Myc-knockdown cells reduced HUVECs tubule formation. Notably, the effect of ADAMTS4-overexpressing derived CM on tubule formation was dramatically reversed by c-Myc depletion (Fig. 5D). These findings suggested a strong functional relationship between ADAMTS4 and c-Myc.

C-Myc was required for ADAMTS4-promoted tumor growth of lung cancer cells in mice

Next, we subcutaneously implanted A549 cells expressing ADAMTS4 and (or) shc-Myc lentiviral vectors into nude mice to further assess the pivotal role of c-Myc in ADAMTS4-mediated lung cancer progression. As shown in Fig. 6A, compared to the NC group, tumor growth was significantly increased by ADAMTS4 overexpression, which was dramatically reversed by down-regulation of c-Myc ($p < 0.001$). Consistently, the tumors tissues isolated from mice in the ADAMTS4 group displayed a larger size and weight, in stark contrast to the results from the ADAMTS4 + shc-Myc group ($p < 0.01$) (Fig. 6B, C), suggesting that ADAMTS4 facilitated lung cancer progression via c-Myc. In addition, we observed an upregulation of Ki-67 in tumors with ADAMTS4 overexpression, a phenomenon that was partly reversed by c-Myc depletion (Fig. 6D). These data confirmed that ADAMTS4 targeted c-Myc to promote in vivo tumorigenicity of lung cancer cells.

ADAMTS4 activated MAPK signaling in lung cancer

To investigate the underlying mechanism by which ADAMTS4 exacerbates lung cancer progression, we performed Gene Set Enrichment Analysis (GSEA) using a publicly available LUAD dataset from TCGA. Our analysis revealed a significant enrichment of co-expressed genes of ADAMTS4 in the mitogen-activated protein

(See figure on next page.)

Fig. 2 ADAMTS4 knockdown inhibited proliferation, migration and angiogenesis in lung cancer. ADAMTS4 knockdown in A549 and NCI-H1299 cells was validated at both, **A** mRNA and, **B** protein levels by qPCR and WB analysis, respectively. (n = 3). **C** ADAMTS4 knockdown in A549 and NCI-H1299 cells inhibited cell viability as shown by Celigo cell counting assays. (n = 3). **D** ADAMTS4 knockdown in A549 and NCI-H1299 cells promoted cell apoptosis as shown by flow cytometry assays. (n = 3). ADAMTS4 knockdown in A549 and NCI-H1299 cells impaired capacities of cell migration as shown by **E** wound healing assays and (F) transwell assays. n = 3. **G** Culture medium (CM) from A549 and **I** NCI-H1299 cells transfected with indicated lentivirus were collected and added to induce HUVECs tube formation. (n = 3). **H** The expression levels of apoptosis, migration and angiogenesis related proteins in A549 and NCI-H1299 cells with or without ADAMTS4 knockdown were detected by Western blot. (n = 3). Results were presented as mean ± SD. *$p < 0.05$, **$p < 0.01$, ***$p < 0.001$

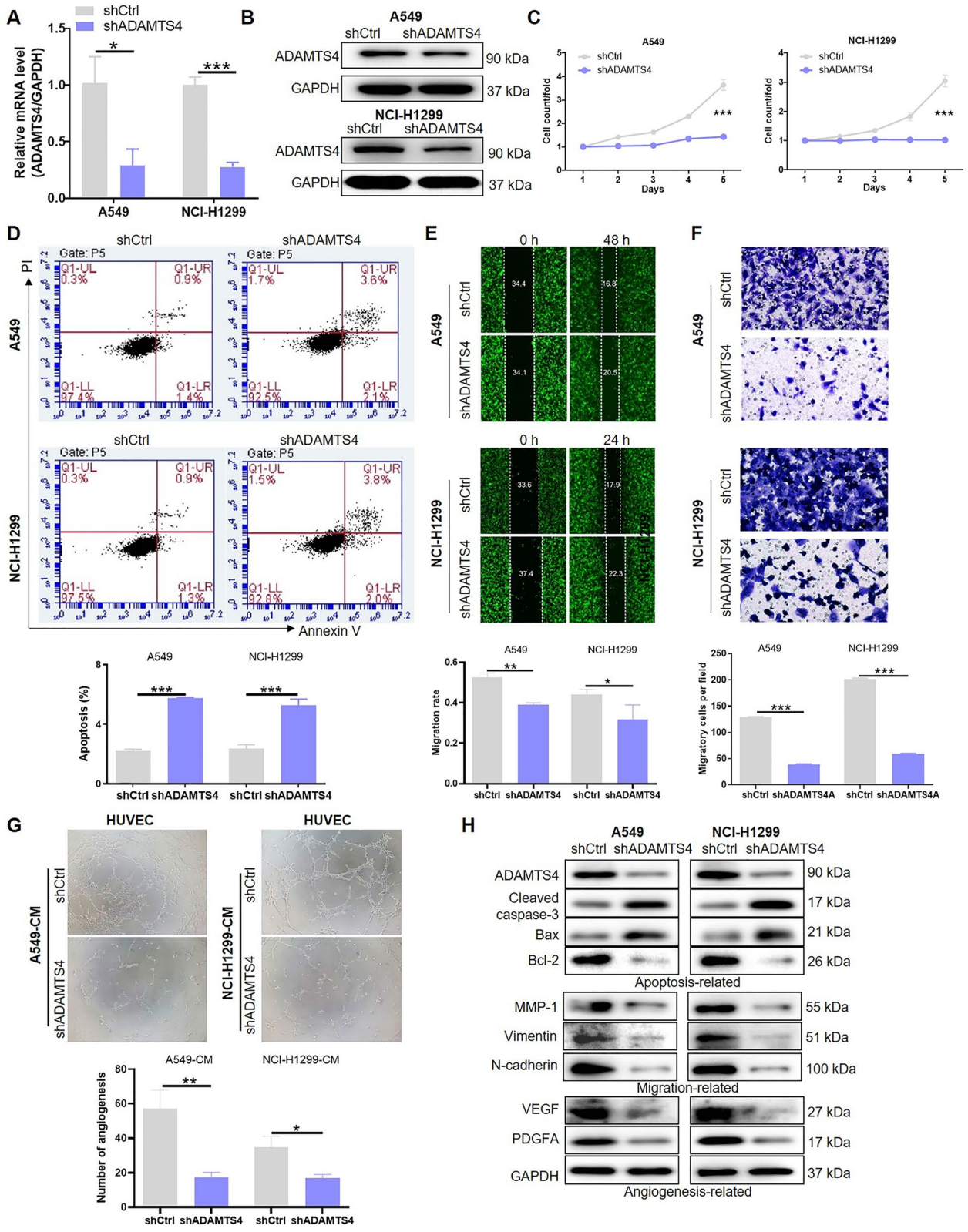

Fig. 2 (See legend on previous page.)

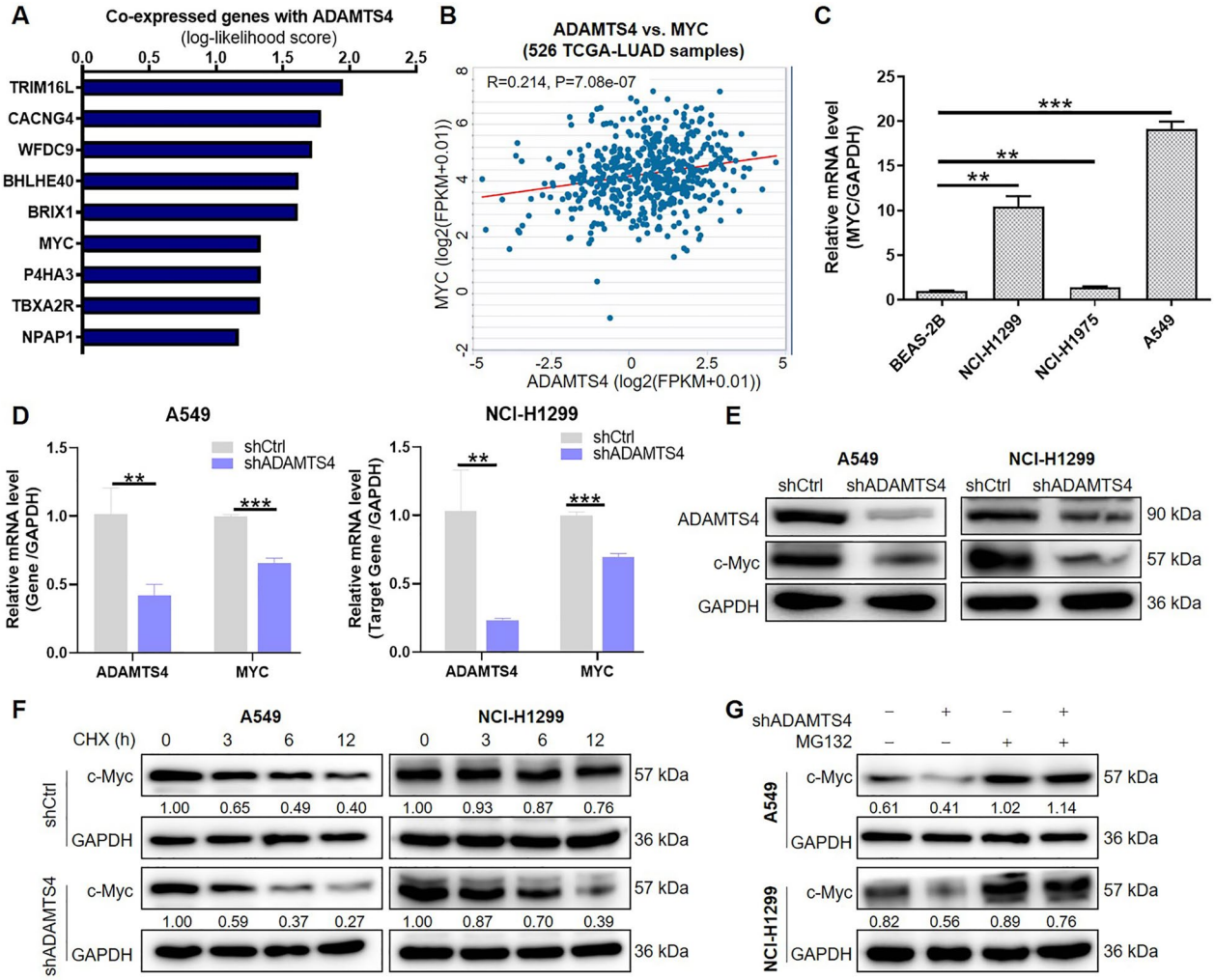

Fig. 3 ADAMTS4 knockdown induced the degradation of c-Myc by ubiquitination in lung cancer. **A** The top 9 of co-expressed genes with ADAMTS4 were identified using Coexpedia. The higher likelihood scores (LLS) represents the greater possibility of co-expression. **B** The co-expression correlation for ADAMTS4 and MYC in LUAD was performed using starbase. **C** Relative mRNA expression level of MYC in lung cancer cell lines NCI-H1299, NCI-H1975, A549 and normal lung epithelial cell BEAS-2B. (n = 3). (D) ADAMTS4 knockdown suppressed the mRNA and **E** protein expression levels in A549 and NCI-H1299 cells. (n = 3). **F** Protein expression of c-Myc in A549 and NCI-H1299 cells transfected with ADAMTS4 knockdown or its negative control lentivirus was detected by WB analysis at indicated times after cyclohexamide (CHX, 20 μmol/L) addition. (n = 3). **G** Protein expression of c-Myc in A549 and NCI-H1299 cells transfected with ADAMTS4 knockdown or its negative control lentivirus and treated with MG132 (20 μg/mL) as indicated was detected by WB analysis. (n = 3). Results were presented as mean ± SD. $^{**}p < 0.01$, $^{***}p < 0.001$

kinase (MAPK) signaling pathway (Fig. 7A), implying the potential implication of the MAPK signaling pathway in ADAMTS4-mediated lung cancer development. Further, western blot assay confirmed that ADAMTS4 overexpression remarkably upregulated c-Myc, along with key molecules of the MAPK signaling pathway, including p-ERK1/2, p-JNK, p-P38. Treatment with MAPK inhibitors or overexpression of WWP2 reduced this effect (Fig. 7B, C), indicating that ADAMTS4/WWP2/c-Myc axis contributes to activation of MAPK signaling pathway in lung cancer. Next, we conducted CCK-8 and cell apoptosis assays to examine whether MAPK signaling pathway contributes to ADAMTS4-mediated malignant phenotypes in lung cancer cells. The results showed that MAPK inhibitor treatment led to a significant inhibition of cell viability in ADAMTS4-overexpressed A549 and NCI-H1299 cells compared with untreated cells ($p < 0.05$) (Fig. 7D). Apoptosis assays suggested that the reduction of apoptotic cell number induced by ADAMTS4 overexpression was partly reversed in A549 and NCI-H1299 cells treated with MAPK inhibitor ($p < 0.05$) (Fig. 7E). Furthermore, we demonstrated that treatment with the MAPK inhibitor resulted in an increase in Bax expression and a decrease in Bcl-2 expression. Importantly, the

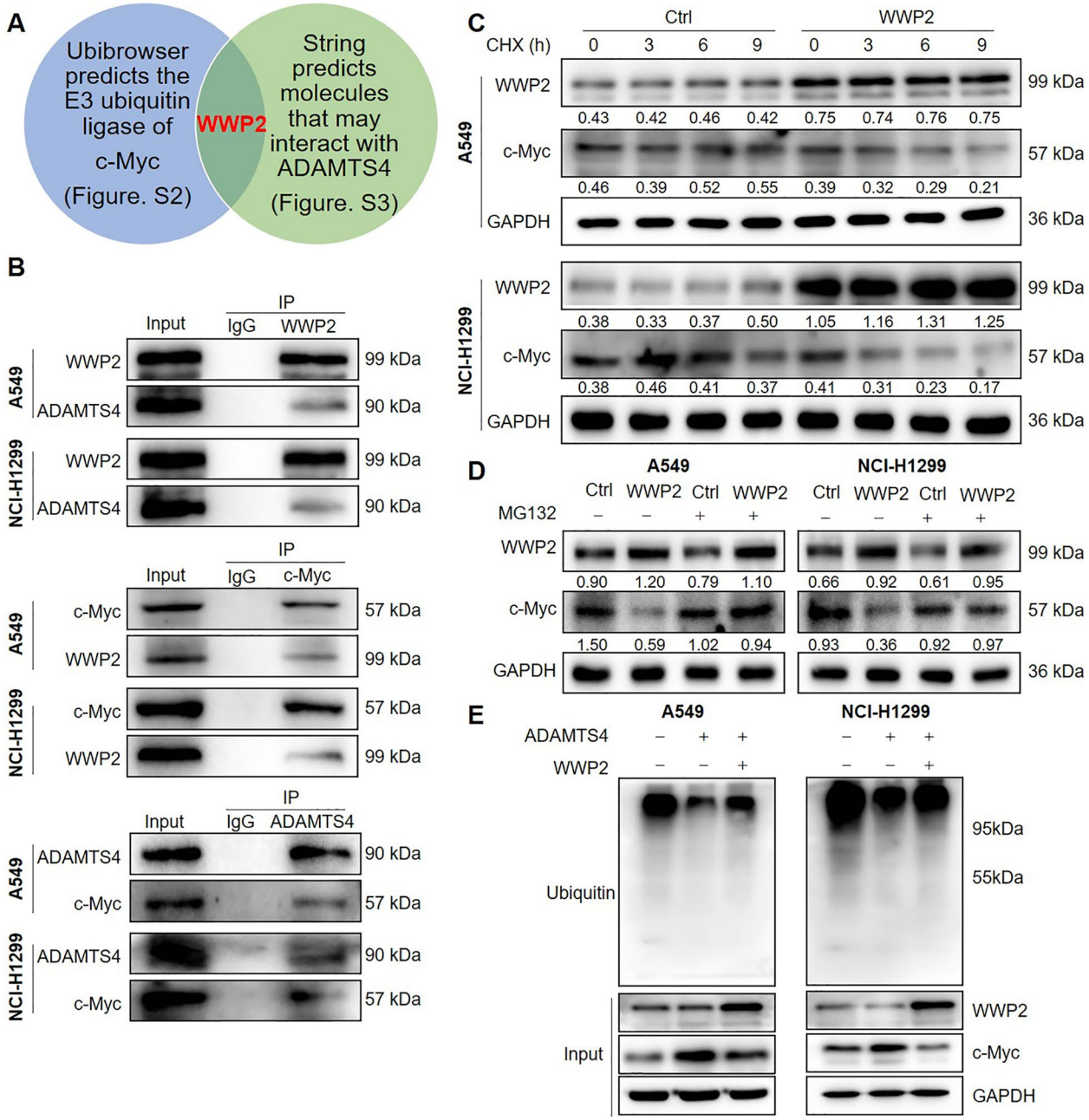

Fig. 4 ADAMTS4 inhibited ubiquitination of c-Myc through WWP2. **A** Venn diagram indicated the potential E3 ubiquitin ligase of c-Myc that may interact with ADAMTS4. **B** Co-IP assays showed endogenous interaction between ADAMTS4, WWP2 and c-Myc in A549 and NCI-H1299 cells. (n = 3). **C** WB analysis showed c-Myc expression in control or WWP2-overexpressed A549 and NCI-H1299 cells treated with CHX. (n = 3). **D** Western blot analysis was performed to assess the protein levels of c-Myc in control and WWP2-overexpressed A549 and NCI-H1299 cells, with or without MG132 treatment. (n = 3). **E** Western blot analysis was conducted to evaluate the ubiquitination levels of c-Myc in A549 and NCI-H1299 cells overexpressing ADAMTS4 alone or co-overexpressing ADAMTS4 and WWP2 simultaneously. (n = 3)

MAPK inhibitor could reverse the effects of ADAMTS4 on the expression of Bax and Bcl-2 proteins (Fig. 7F). Altogether, our findings establish the involvement of the MAPK signaling pathway in ADAMTS4-mediated lung cancer progression.

Discussion

Lung cancer is a prevalent malignant tumor and remains the primary cause of cancer-related deaths globally [1]. While the preferred therapeutic approach for early-stage patients involves resection combined with adjuvant

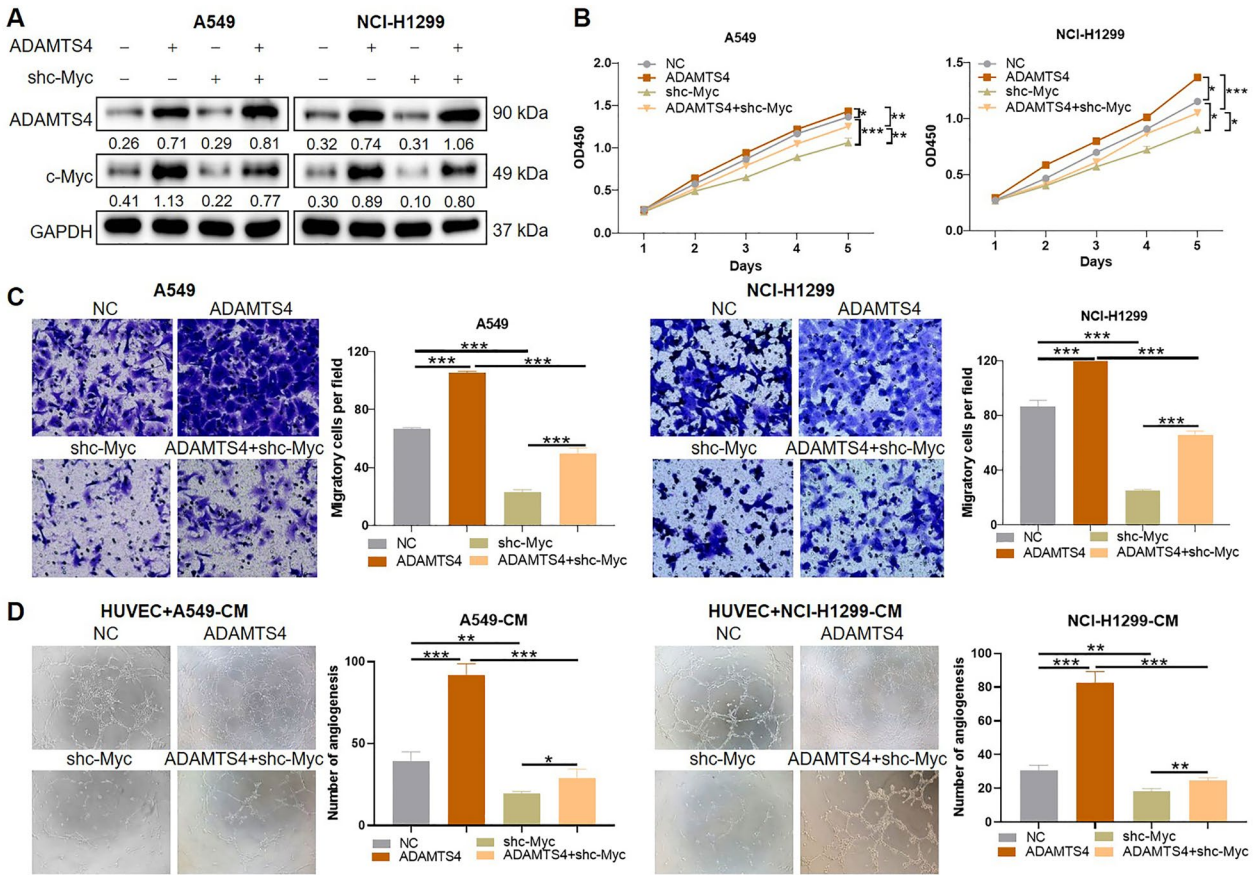

Fig. 5 The function of ADAMTS4 in promoting proliferation and migration relied on c-Myc. The A549 and NCI-H1299 cells were co-transfected with ADAMTS4-overexpressing and c-Myc-silencing negative vectors (NC), ADAMTS4-overexpressing lentivirus and c-Myc-silencing negative vectors (ADAMTS4), ADAMTS4-overexpressing negative vector and c-Myc-silencing lentivirus (shc-Myc), and ADAMTS4-overexpressing lentivirus and c-Myc-silencing lentivirus (ADAMTS4 + shc-Myc), respectively. 48 h later, cells were harvested for **A** western blot analysis of ADAMTS4 and c-Myc expression. GAPDH used as an internal control. (n = 3). **B** Detection of cell viability by CCK-8 assays. (n = 3). **C** Evaluation of cell migration ability by transwell assays. (n = 3). **D** Culture medium (CM) from A549 and NCI-H1299 cells transfected with indicated lentivirus were collected and added to induce HUVECs tube formation. Representative tube structures of HUVECs cells were shown and the numbers of angiogenesis were quantified. (n = 3). Results were presented as mean ± SD. *$p < 0.05$, **$p < 0.01$, ***$p < 0.001$

chemotherapy, this strategy comes with notable toxicities [35]. Moreover, the current targeted agents for lung cancer face challenges such as modest efficacy and limited applicability to specific populations [36, 37]. Consequently, revealing the pathogenesis of lung cancer and searching for a promising therapeutic target are of great significance for improving the survival of lung cancer patients.

ECM is an intricate network of large molecules secreted by cells into the extracellular stroma. It exerts pleiotropic effects, including structural support, anchorage, cell signaling, morphogenesis, cell survival, and cell death. Aberrant production and regulation of ECM are implicated in various diseases such as fibrosis, myopathies, diabetes, and cancer [38]. The proteinase ADAMTS4, responsible for controlling the structure and function of ECM, is implicated in tissue destructions, contributing to conditions like arthritis or cancers [39, 40]. The upregulation of ADAMTS4 has been identified in colorectal cancer [15, 16], Ewing's sarcoma [17], and is associated with poor prognosis. Recently, ADAMTS4 was reported to mediate fibroblast activation-induced lung damage [41], yet its involvement in lung cancer progression remains unclear. In our study, we assessed the protein expression of ADAMTS4 in samples from lung cancer patients, revealing high levels. Significantly, upregulation of ADAMTS4 was more significantly in advanced lung cancer and correlated with shortened OS, indicating ADAMTS4 as a promising biomarker for lung cancer progression. Proliferation and migration, predominant factors driving tumor dissemination [42], were notably elevated. Using loss-of-function strategies, we further demonstrated that ADAMTS4 knockdown apparently inhibited cell viability and migration

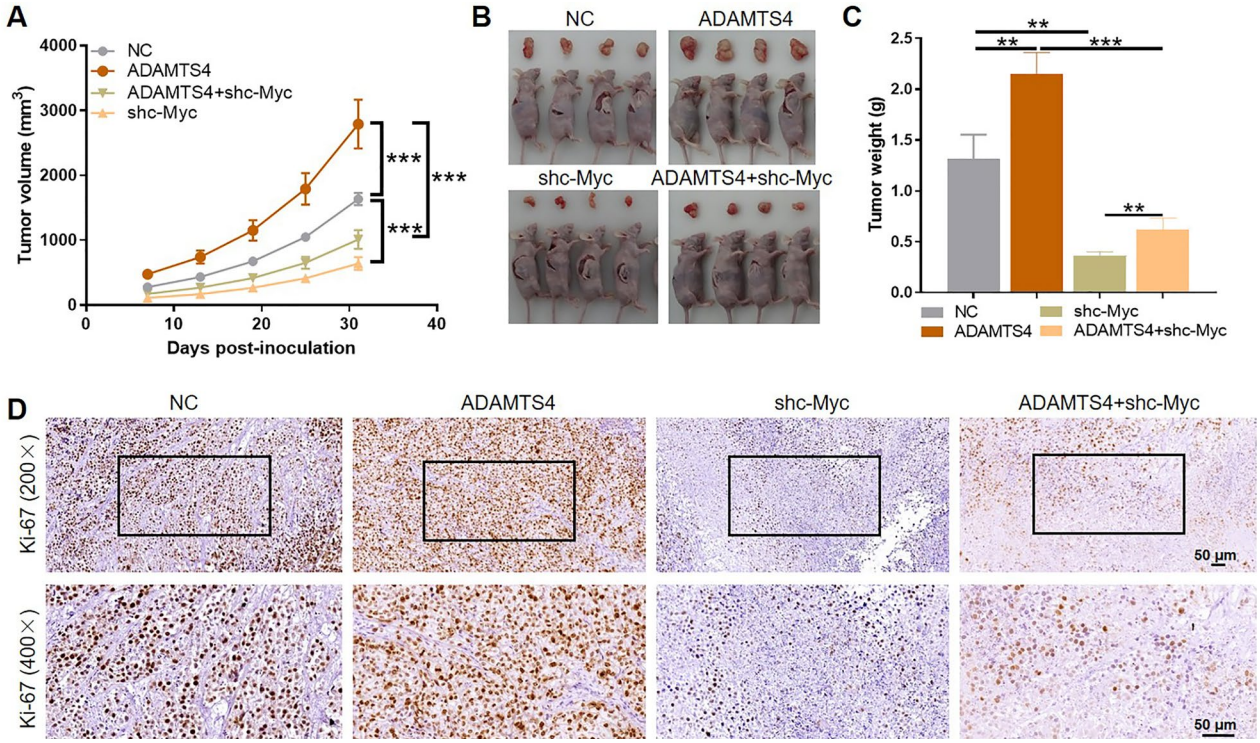

Fig. 6 C-Myc was required for ADAMTS4-promoted tumor growth of lung cancer cells in mice. **A** The ADAMTS4-overexpressing lentivirus and c-Myc-silencing A549 cells were respectively or simultaneously injected into flanks of BALB/c nude mice. 7 days later, the tumor sizes were monitored once every 6 days, and the tumor volumes were calculated. (n = 4 mice per group). **B** After 31 days, all tumor tissues isolated from mice as well as the mice were photographed, and **C** tumor weight was quantified. (n = 4 mice per group). **D** The expression levels of Ki-67 protein in tumors of indicated groups were detected by IHC staining. (n = 4 mice per group). Results were presented as mean ± SD. $^{**}p < 0.01$, $^{***}p < 0.001$

while promoting apoptosis in A549 and NCI-H1299 cells. Moreover, the inhibitory effect of ADAMTS4-knockdown CM on HUVEC tubule formation further supported ADAMTS4's oncogenic role in lung cancer development.

The transcription factor c-Myc is intricately involved in regulating cell growth, survival, differentiation, metabolism and apoptosis, exhibits constitutive and aberrant expression in more than 70% of human cancers [43]. Herein, we identified c-Myc as one of the co-expressed genes alongside ADAMTS4, demonstrating a positive correlation between their expressions. Consistent with ADAMTS4, elevated levels of c-Myc were observed in A549 and NCI-H1299 cells. Further analysis validated that depletion of ADAMTS4 significantly decreased both mRNA and protein expression levels of c-Myc, prompting the hypothesis that ADAMTS4 might accelerate lung cancer progression through c-Myc, although the underlying molecular mechanism remained elusive. More importantly, previous researchers have suggested the short half-life and inherent instability of c-Myc protein, leading to various posttranslational modifications for its regulation [44, 45]. Among these modifications, the delicate balance of ubiquitination and deubiquitination

(See figure on next page.)

Fig. 7 ADAMTS4 activated MAPK signaling in lung cancer. **A** GSEA indicated that the co-expressed genes of ADAMTS4 were enriched in MAPK signaling pathway. **B** Western blot assay confirmed the activation of MAPK signaling pathway in NCI-H1299 cells upon ADAMTS4 overexpression. GAPDH served as the internal reference. (n = 3). **C** Western blot assay indicated that WWP2 attenuated the activation of MAPK signaling pathway induced by ADAMTS4 overexpression. GAPDH served as the internal reference. (n = 3). **D** CCK-8 assays were performed to examine the effect of ADAMTS4 or (and) MAPK inhibitor, HY-12839 (10 μM), on cell viability of A549 and NCI-H1299 cells. (n = 3). **E** Flow cytometry was used for detecting the effect of ADAMTS4 or (and) MAPK inhibitor on cell apoptosis of A549 and NCI-H1299 cells. (n = 3). **F** Relative protein expression levels of cleaved caspase-3, Bax and Bcl-2 expression in A549 and NCI-H1299 cells. GAPDH served as the internal reference. (n = 3). Results were presented as mean ± SD. $^{*}p < 0.05$, $^{**}p < 0.01$, $^{***}p < 0.001$

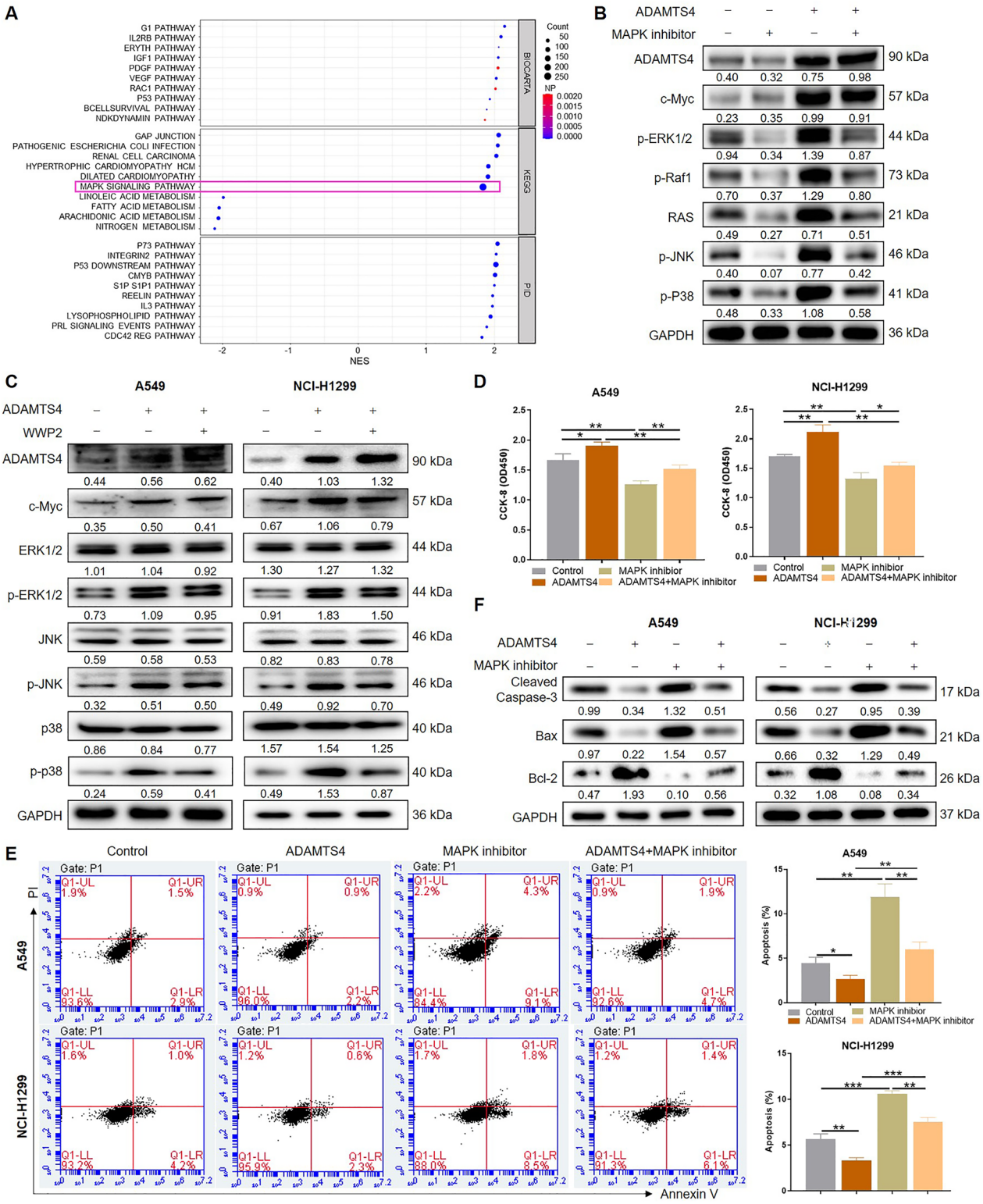

Fig. 7 (See legend on previous page.)

emerges as a pivotal factor in regulating c-Myc stabilization and activation [44]. For example, The c-Box and ubiquitin binding domain (UBA) regions of USP5 interact with the c-Myc protein, thereby inhibiting K48-linked polyubiquitination of c-Myc. Additional studies have revealed that METTL5 regulates the translation of USP5, influencing c-Myc ubiquitination [46]. WBC100 targets the nuclear localization signal 1 (NLS1) and basic nuclear localization signal 2 (NLS2) regions of c-Myc, triggering its degradation via the 26S proteasome pathway mediated by the ubiquitin E3 ligase CHIP, ultimately inducing apoptosis in cancer cells [47]. Furthermore, RNF130 has been identified as promoting ubiquitination and degradation of c-Myc [48]. In our study, we evaluated the effects of ADAMTS4 on c-Myc protein stability, revealing that ADAMTS4 knockdown remarkably decreased the stability of c-Myc protein in lung cancer cells. In addition, we identified E3 ubiquitin ligase WWP2 mediated the regulatory effect of ADAMTS4 on c-Myc protein stability. ADAMTS4 may upregulate c-Myc expression by inhibiting WWP2-mediated ubiquitination of c-Myc. Furthermore, the rescue assays provided that the promotive cell viability and migratory effects by ADAMTS4 overexpression in lung cancer, as well as in vivo tumor growth, were dependent on c-Myc. In addition, Baudino et al. demonstrated the essential role of c-Myc in vasculogenesis and angiogenesis during tumor progression using c-myc$^{-/-}$ mice [49]. We next investigated the potential role of ADAMTS4 in promoting angiogenesis in lung cancer through its interaction with c-Myc. Our findings revealed that the CM from lung cancer cells overexpressing ADAMTS4 remarkably enhanced tube formation in HUVEC cells. In contrast, groups with knockdown of either ADAMTS4 or c-Myc exhibited diminished tube formation capabilities. Notably, the pro-angiogenic effect of the CM derived from ADAMTS4-overexpressing cells was substantially reversed upon depletion of c-Myc. This observation aligns with a prior study by Rao et al. indicating that ADAMTS4 exhibited promotive role in B16 melanoma growth and angiogenesis in mice [18]. Thus, our results suggest that ADAMTS4 might induce angiogenesis in lung cancer in a c-Myc depended manner, providing insight into the mechanistic underpinnings of its role in facilitating lung cancer progression.

The Mitogen-Activated Protein Kinase (MAPK) signaling pathway comprises three principal modules-ERK, JNK, and p38-which control cellular processes such as cell proliferation, differentiation, survival, apoptosis [50], and angiogenesis [51]. Dysregulation of the MAPK pathway has been implicated in various human diseases, including cancer [50, 52]. In the context of lung cancer, multiple studies have reported aberrant activation of MAPK signaling pathways in tumor tissues, indicating its significance in the pathogenesis of this malignancy [53, 54]. Herein, we demonstrated that ADAMTS4/WWP2/c-Myc axis contributes to activation of MAPK signaling pathway in lung cancer. This activation, in turn, promotes a malignant proliferative phenotype in lung cancer cells, thereby accelerating tumor progression.

In conclusion, our study offers the initial glimpse into the spectrum of malignant traits orchestrated by ADAMTS4 in lung cancer, including proliferation, migration, anti-apoptosis and angiogenesis. Mechanistically, we elucidated that ADAMTS4 drives tumorigenesis by regulating the stability of c-Myc protein and activating the MAPK signaling pathway. Most importantly, we revealed ADAMTS4 as a promising biomarker and therapeutic target for lung cancer patients, supported by the analysis of human tumor samples and comprehensive functional explorations.

Supplementary Information

The online version contains supplementary material available at https://doi.org/10.1186/s13062-024-00512-y.

Supplementary Material 1: Figure S1. Screening for effective interference targets. (A) Three shRNAs targeting ADAMTS4 and (B) MYC were used to transfect NCI-H1299 cells, and the knockdown efficiency was determined by qPCR assays. (n = 3). GAPDH served as the internal reference. Results were presented as mean ± SD. *p < 0.05, **p < 0.01

Supplementary Material 2: Figure S2. Potential E3 ubiquitin ligases of c-Myc were predicted using Ubibrowser

Supplementary Material 3: Figure S3. String predicts molecules that may interact with ADAMTS4

Supplementary Material 4 Note: The version of Supplementary Material 4 uploaded in the online proofreading system is outdated. An updated version has been submitted alongside this manuscript. Please refer to the latest attachment for the most accurate and comprehensive information.

Supplementary Material 5

Acknowledgements
None.

Author contributions
Xingxiang Pu designed this project. Wei Zhai, Wensheng Yang, Xuelian Xiao, Jing Ge, Yu Zhou, Kang Wu and Shiya Luo conducted experiments. Kelin She, Yi Kong and Lin Wu performed the data analysis. Wei Zhai wrote the manuscript which was checked by Xingxiang Pu. All authors have confirmed the submission of this manuscript.

Funding
This study was supported by Hunan Provincial Natural Science Foundation of China (No. 2024JJ9137), Hunan Cancer Hospital Climb Plan (No. YF2020005), Beijing Xisike Clinical Oncology Research Foundation (No. Y-XD202001-0215), Wu JiePing Medical Fund (No. 320.6750.2023-05-43), the Science and Technology Innovation Program of Hunan Province (No. 2023SK4024), Changsha Municipal Natural Science Foundation (No. Kq2403119) and funds from the University Cancer Foundation via Sister Institution Network Fund of the University of Texas MD Anderson Cancer Center.

Data availability
The data generated in this study are available within the article and its supplementary data files.

Declarations

Ethics approval and consent to participate
The study involved human tissue samples use and animal experiments performing were all approved by the Ethics Committee of Hunan Cancer Hospital/The Affiliated Cancer Hospital of Xiangya school of Medicine, Central South University. The informed consents were obtained from patients. All the methods and procedures performed during this study were in accordance with relevant regulation and guidelines.

Consent for publication
Not applicable.

Competing interests
The authors declare that they have no conflict of interest.

Author details
[1]Department of Thoracic Surgery, Union Hospital, Tongji Medical College, Huazhong University of Science and Technology, No. 1277, Jiefang Road, Wuhan 430030, Hubei, China. [2]Department of Thoracic Surgery, The Affiliated Shaoyang Hospital, Hengyang Medical School, University of South China, No. 36, Hongqi Road, Daxiang District, Shaoyang 422000, Hunan, China. [3]Department of Geriatrics and Institute of Geriatrics, Union Hospital, Tongji Medical College, Huazhong University of Science and Technology, No.1277, Jiefang Road, Wuhan 430030, Hubei, China. [4]Department of Medical Administration, Hunan Cancer Hospital/The Affiliated Cancer Hospital of Xiangya School of Medicine, Central South University, No. 283 Tongzipo Road, Yuelu District, Changsha 410013, Hunan, China. [5]Sansure Biotech Inc.,, No. 680, Lusong Road, Yuelu District, Changsha 410205, Hunan, China. [6]Department of Thoracic Surgery, Hunan Provincial Pecople's Hospital, The First Affiliated Hospital of Huan Nomal University, No. 61, Jiefang West Road, Furong District, Changsha 410013, Hunan, China. [7]Department of Medical Oncology, Lung Cancer and Gastrointestinal Unit, Hunan Cancer Hospital/The Affiliated Cancer Hospital of Xiangya School of Medicine, Central South University, No. 283, Tongzipo Road, Yuelu District, Changsha 410013, Hunan, China.

Received: 31 May 2023 Accepted: 8 August 2024
Published online: 16 October 2024

References

1. Oliver AL. Lung cancer: epidemiology and screening. Surg Clin North Am. 2022;102:335–44.
2. Liang J, Guan X, Bao G, Yao Y, Zhong X. Molecular subtyping of small cell lung cancer. Semin Cancer Biol. 2022;86:450–62.
3. Lee JH, Saxena A, Giaccone G. Advancements in small cell lung cancer. Semin Cancer Biol. 2023;93:123–8.
4. Lovly CM. Expanding horizons for treatment of early-stage lung cancer. N Engl J Med. 2022;386:2050–1.
5. Chen P, Liu Y, Wen Y, Zhou C. Non-small cell lung cancer in China. Cancer Commun (Lond). 2022;42:937–70.
6. Hendriks LE, Kerr KM, Menis J, Mok TS, Nestle U, Passaro A, Peters S, Planchard D, Smit EF, Solomon BJ, et al. Non-oncogene-addicted metastatic non-small-cell lung cancer: ESMO Clinical Practice Guideline for diagnosis, treatment and follow-up. Ann Oncol. 2023;34:358–76.
7. Meijer JJ, Leonetti A, Airo G, Tiseo M, Rolfo C, Giovannetti E, Vahabi M. Small cell lung cancer: novel treatments beyond immunotherapy. Semin Cancer Biol. 2022;86:376–85.
8. Johnson M, Garassino MC, Mok T, Mitsudomi T. Treatment strategies and outcomes for patients with EGFR-mutant non-small cell lung cancer resistant to EGFR tyrosine kinase inhibitors: Focus on novel therapies. Lung Cancer. 2022;170:41–51.
9. Hirsch FR, Scagliotti GV, Mulshine JL, Kwon R, Curran WJ Jr, Wu YL, Paz-Ares L. Lung cancer: current therapies and new targeted treatments. Lancet. 2017;389:299–311.
10. Apte SS. ADAMTS proteins: concepts, challenges, and prospects. Methods Mol Biol. 2020;2043:1–12.
11. Satz-Jacobowitz B, Hubmacher D. The quest for substrates and binding partners: a critical barrier for understanding the role of ADAMTS proteases in musculoskeletal development and disease. Dev Dyn. 2021;250:8–26.
12. Evans DR, Green JS, Fahiminiya S, Majewski J, Fernandez BA, Deardorff MA, Johnson GJ, Whelan JH, Hubmacher D, Apte SS, et al. A novel pathogenic missense ADAMTS17 variant that impairs secretion causes Weill-Marchesani Syndrome with variably dysmorphic hand features. Sci Rep. 2020;10:10827.
13. Wunnemann F, Ta-Shma A, Preuss C, Leclerc S, van Vliet PP, Oneglia A, Thibeault M, Nordquist E, Lincoln J, Scharfenberg F, et al. Loss of ADAMTS19 causes progressive non-syndromic heart valve disease. Nat Genet. 2020;52:40–7.
14. Matsuzaki M, Yokoyama M, Yoshizawa Y, Kaneko N, Naito H, Kobayashi H, Korenaga A, Sekiya S, Ikemura K, Opoku G, et al. ADAMTS4 is involved in the production of the Alzheimer disease amyloid biomarker APP669-711. Mol Psychiatry. 2023;28:1802–12.
15. Shang XQ, Liu KL, Li Q, Lao YQ, Li NS, Wu J. ADAMTS4 is upregulated in colorectal cancer and could be a useful prognostic indicator of colorectal cancer. Rev Assoc Med Bras. 1992;2020(66):42–7.
16. Chen J, Luo Y, Zhou Y, Qin S, Qiu Y, Cui R, Yu M, Qin J, Zhong M. Promotion of tumor growth by ADAMTS4 in colorectal cancer: focused on macrophages. Cell Physiol Biochem. 2018;46:1693–703.
17. Minobe K, Ono R, Matsumine A, Shibata-Minoshima F, Izawa K, Oki T, Kitaura J, Iino T, Takita J, Iwamoto S, et al. Expression of ADAMTS4 in Ewing's sarcoma. Int J Oncol. 2010;37:569–81.
18. Rao N, Ke Z, Liu H, Ho CJ, Kumar S, Xiang W, Zhu Y, Ge R. ADAMTS4 and its proteolytic fragments differentially affect melanoma growth and angiogenesis in mice. Int J Cancer. 2013;133:294–306.
19. Dang CV. MYC on the path to cancer. Cell. 2012;149:22–35.
20. Kress TR, Sabo A, Amati B. MYC: connecting selective transcriptional control to global RNA production. Nat Rev Cancer. 2015;15:593–607.
21. Brooks TA, Hurley LH. Targeting MYC expression through G-quadruplexes. Genes Cancer. 2010;1:641–9.
22. Fatma H, Maurya SK, Siddique HR. Epigenetic modifications of c-MYC: role in cancer cell reprogramming, progression and chemoresistance. Semin Cancer Biol. 2022;83:166–76.
23. Gao FY, Li XT, Xu K, Wang RT, Guan XX. c-MYC mediates the crosstalk between breast cancer cells and tumor microenvironment. Cell Commun Signal. 2023;21:28.
24. Ala M. Target c-Myc to treat pancreatic cancer. Cancer Biol Ther. 2022;23:34–50.
25. Dhanasekaran R, Deutzmann A, Mahauad-Fernandez WD, Hansen AS, Gouw AM, Felsher DW. The MYC oncogene—the grand orchestrator of cancer growth and immune evasion. Nat Rev Clin Oncol. 2022;19:23–36.
26. Llombart V, Mansour MR. Therapeutic targeting of "undruggable" MYC. EBioMedicine. 2022;75: 103756.
27. Ma Y, Ma L, Guo Q, Zhang S. Expression of bone morphogenetic protein-2 and its receptors in epithelial ovarian cancer and their influence on the prognosis of ovarian cancer patients. J Exp Clin Cancer Res. 2010;29:85.
28. Zhi T, Jiang K, Xu X, Yu T, Zhou F, Wang Y, Liu N, Zhang J. ECT2/PSMD14/PTTG1 axis promotes the proliferation of glioma through stabilizing E2F1. Neuro Oncol. 2019;21:462–73.
29. Zhou H, Liu Y, Zhu R, Ding F, Wan Y, Li Y, Liu Z. FBXO32 suppresses breast cancer tumorigenesis through targeting KLF4 to proteasomal degradation. Oncogene. 2017;36:3312–21.
30. Gentile MT, Pastorino O, Bifulco M, Colucci-D'Amato L. HUVEC tube-formation assay to evaluate the impact of natural products on angiogenesis. J Vis Exp. 2019. https://doi.org/10.3791/58591.
31. Liu P, Tang H, Chen B, He Z, Deng M, Wu M, Liu X, Yang L, Ye F, Xie X. miR-26a suppresses tumour proliferation and metastasis by targeting metadherin in triple negative breast cancer. Cancer Lett. 2015;357:384–92.
32. Popper HH. Progression and metastasis of lung cancer. Cancer Metastasis Rev. 2016;35:75–91.
33. Duffy MJ, O'Grady S, Tang M, Crown J. MYC as a target for cancer treatment. Cancer Treat Rev. 2021;94: 102154.
34. Farrell AS, Sears RC. MYC degradation. Cold Spring Harb Perspect Med. 2014;4:a014365.

35. Muthusamy B, Patil PD, Pennell NA. Perioperative systemic therapy for resectable non-small cell lung cancer. J Natl Compr Canc Netw. 2022;20:953–61.
36. Li Y, Wu X, Yang P, Jiang G, Luo Y. Machine learning for lung cancer diagnosis, treatment, and prognosis. Genom Proteom Bioinf. 2022;20:850–66.
37. Liu SY, Liu SM, Zhong WZ, Wu YL. Targeted therapy in early stage non-small cell lung cancer. Curr Treat Options Oncol. 2022;23:1169–84.
38. Valdoz JC, Johnson BC, Jacobs DJ, Franks NA, Dodson EL, Sanders C, Cribbs CG, Van Ry PM. The ECM: to scaffold, or not to scaffold, that is the question. Int J Mol Sci. 2021;22:12690.
39. Rose KWJ, Taye N, Karoulias SZ, Hubmacher D. Regulation of ADAMTS proteases. Front Mol Biosci. 2021;8: 701959.
40. Kelwick R, Desanlis I, Wheeler GN, Edwards DR. The ADAMTS (A Disintegrin and Metalloproteinase with Thrombospondin motifs) family. Genome Biol. 2015;16:113.
41. Boyd DF, Allen EK, Randolph AG, Guo XJ, Weng Y, Sanders CJ, Bajracharya R, Lee NK, Guy CS, Vogel P, et al. Exuberant fibroblast activity compromises lung function via ADAMTS4. Nature. 2020;587:466–71.
42. Lv X, Lv Y, Dai X. Lactate, histone lactylation and cancer hallmarks. Expert Rev Mol Med. 2023;25: e7.
43. Madden SK, de Araujo AD, Gerhardt M, Fairlie DP, Mason JM. Taking the Myc out of cancer: toward therapeutic strategies to directly inhibit c-Myc. Mol Cancer. 2021;20:3.
44. Sun XX, Li Y, Sears RC, Dai MS. Targeting the MYC ubiquitination-proteasome degradation pathway for cancer therapy. Front Oncol. 2021;11: 679445.
45. Hann SR. Role of post-translational modifications in regulating c-Myc proteolysis, transcriptional activity and biological function. Semin Cancer Biol. 2006;16:288–302.
46. Xia P, Zhang H, Lu H, Xu K, Jiang X, Jiang Y, Gongye X, Chen Z, Liu J, Chen X, et al. METTL5 stabilizes c-Myc by facilitating USP5 translation to reprogram glucose metabolism and promote hepatocellular carcinoma progression. Cancer Commun (Lond). 2023;43:338–64.
47. Xu Y, Yu Q, Wang P, Wu Z, Zhang L, Wu S, Li M, Wu B, Li H, Zhuang H, et al. A selective small-molecule c-Myc degrader potently regresses lethal c-Myc overexpressing tumors. Adv Sci (Weinh). 2022;9: e2104344.
48. Zhang J, Chen W, Du J, Chu L, Zhou Z, Zhong W, Liu D, Huang H, Huang Y, Qiao Y, et al. RNF130 protects against pulmonary fibrosis through suppressing aerobic glycolysis by mediating c-myc ubiquitination. Int Immunopharmacol. 2023;117: 109985.
49. Baudino TA, McKay C, Pendeville-Samain H, Nilsson JA, Maclean KH, White EL, Davis AC, Ihle JN, Cleveland JL. c-Myc is essential for vasculogenesis and angiogenesis during development and tumor progression. Genes Dev. 2002;16:2530–43.
50. Ullah R, Yin Q, Snell AH, Wan L. RAF-MEK-ERK pathway in cancer evolution and treatment. Semin Cancer Biol. 2022;85:123–54.
51. Yuan R, Li Y, Yang B, Jin Z, Xu J, Shao Z, Miao H, Ren T, Yang Y, Li G, et al. LOXL1 exerts oncogenesis and stimulates angiogenesis through the LOXL1-FBLN5/alphavbeta3 integrin/FAK-MAPK axis in ICC. Mol Ther Nucleic Acids. 2021;23:797–810.
52. Lee S, Rauch J, Kolch W. Targeting MAPK signaling in cancer: mechanisms of drug resistance and sensitivity. Int J Mol Sci. 2020;21:1102.
53. Wei S, Zhao Q, Zheng K, Liu P, Sha N, Li Y, Ma C, Li J, Zhuo L, Liu G, et al. GFAT1-linked TAB1 glutamylation sustains p38 MAPK activation and promotes lung cancer cell survival under glucose starvation. Cell Discov. 2022;8:77.
54. Liu Z, Zhao M, Jiang X, Zhang Y, Zhang S, Xu Y, Ren H, Su H, Wang H, Qiu X. Upregulation of KLHL17 promotes the proliferation and migration of non-small cell lung cancer by activating the Ras/MAPK signaling pathway. Lab Invest. 2022;102:1389–99.

Publisher's Note